

# **Nitrogen in SL/RN Direct Reduced Iron: Origin and Effect on nitrogen control in EAF steelmaking**

Markus W. Erwee<sup>1</sup> and P. Chris Pistorius<sup>2</sup>

<sup>1</sup> Department of Materials Science and Metallurgical Engineering  
University of Pretoria, South Africa, 0002  
Phone: +27 (0) 12 420 4550  
Fax: +27 (0) 12 362 5304  
E-mail: markus.erwee@up.ac.za

<sup>2</sup> Department of Materials Science and Engineering  
Carnegie Mellon University, Pittsburgh, PA 15213  
United States of America  
Phone: +1 (412) 268 7248  
Fax: +1 (412) 268 7247  
E-mail: pistorius@cmu.edu

## **Abstract**

In the steel plant considered here, direct reduced iron (DRI), produced by the coal-based SL/RN process, makes up 50% or more of the total iron charge. SL/RN DRI samples from a kiln cooler had high nitrogen contents (50-250ppm, depending on particle size), contributing to elevated nitrogen levels in liquid steel produced in the EAFs. The proposed mechanism of nitriding of SL/RN DRI involves gaseous nitrogen (present within the rotary cooler) diffusion into the solids bed, and is supported by a simple diffusion model. A strong correlation was found between the melt-in carbon content of the liquid steel and the final tap nitrogen content, with melt-in carbon of 0.3% C or higher resulting in nitrogen levels below 50 ppm at tap, even when charging DRI material that is high in nitrogen.

Keywords: SL/RN, Rotary Kiln, Direct Reduced Iron, Nitrogen Control, Electric Steelmaking

## **Introduction**

Direct reduced iron (DRI) has become a valuable feedstock to the electric arc furnace (EAF). In the last ten years, annual worldwide production of DRI has increased by approximately 60% to 70 Mt in 2010<sup>1</sup>. DRI production is dominated by gas-based reductant processes like MIDREX (58% of world DRI produced in 2010),<sup>1</sup> but coal-based reduction remains important in both India and South Africa – where coal is relatively inexpensive and gaseous reductants are not readily available. In total, approximately 26% of DRI is produced in rotary-kiln coal-based processes such as the Stelco-Lurgi/Republic-National (SL/RN) rotary kiln process.<sup>1</sup> In this process, approximately 1.5 tons of lump ore (-31.5+3.15mm), 800 kg of coal and 40 kg of dolomite are fed to a kiln to produce 1 ton of DRI. At the kiln exit, the transfer of material is through a transfer chute (closed off from the atmosphere) through which the material falls into a rotary cooler. The DRI produced in the kiln exits at

approximately 1000°C (residence time in the kiln is approximately 12 hours) and is cooled in a water-cooled rotary cooler (up to 80 meters long, residence time approximately 2 hours), to approximately 100°C. The kiln atmosphere consists mainly of nitrogen, carbon dioxide and water vapor; the atmosphere in the cooler is expected to be mainly nitrogen.

Nitrogen control in EAF steelmaking can be successfully achieved by applying three principles: using feed materials with low nitrogen levels; preventing absorption of nitrogen from the atmosphere and by removing nitrogen during or after steelmaking.<sup>2</sup>

Many authors have investigated the benefits of having sufficient amounts of carbon in DRI to reduce nitrogen levels in liquid steel during electric steelmaking<sup>3,4</sup>. Carbon, when present at sufficient levels (approx. 1.8%), yielded substantial improvements in slag foaming properties<sup>5</sup> by the promotion of carbon boil. In addition, trials have also been run on injection of fine DRI material into steel melts to essentially start the carbon boil within the steel melt<sup>6</sup>. There needs to be a balance between the amounts of carbon and oxygen present in DRI (1% C balances around 6% FeO, yielding CO and metallic iron when heated), to promote slag foaming and hence shielding the bath from the atmosphere.

Goldstein et al.<sup>4</sup> showed that when DRI is dropped into a metal-slag melt, that DRI does not necessarily penetrate the metal, but rather floats on top of the melt (at the slag/metal interface), releasing carbon as carbon monoxide gas, foaming the slag, but not increasing the carbon content of the melt. This implies that the use of DRI to increase the carbon content of a steel melt is limited (if at all possible), yet various plants appear to benefit from using DRI with higher carbon content than that produced via the rotary kiln route.

Since the SL/RN process is a solid-state reduction process, with solid carbon as reductant, little carbon dissolves in the sponge iron. The carbon content of DRI produced at the plant considered in this work is less than 0.15% C<sup>7</sup>, considerably lower than that of DRI produced by gaseous reduction processes (such as MIDREX), for which the carbon content of the DRI is between 1 and 2.5%<sup>8</sup> (due to carburisation during cooling in a methane/hydrogen mixture after reduction).

## **Plant description**

The plant of which production data were analysed in this work uses a large proportion of SL/RN DRI in the feed to the electric furnaces. Typical degree of metallisation of the DRI is 88-90%.

It was found that the nitrogen content of liquid steel tapped was often in excess of 80 parts per million (ppm) by mass, higher than expected (compared with plants using gas-based DRI). The aim of the investigation summarised here was to identify reasons for the high nitrogen tap content, and to suggest possible remedial measures. As background, a short description of the production process is presented first.

The electric steel plant produces crude steel (with roughly 0.03%C) using three electric arc furnaces mainly from scrap and DRI, tapped at approximately 1630°C. Each furnace has a capacity of 180 tons, tapping on average 155 tons per heat. On average, the charge mixture is 30% scrap, 50% DRI (the ratio between DRI charged in the basket and that which is charged through the roof is typically 1:5), 10% hot metal (from a blast furnace) with the remaining

10% including pool iron and other high-carbon material. A typical timeline for steel production in these furnaces is shown in Fig. 1; in more detail, the process steps are as follows.

Hot metal – if used – is charged first into the 15-30 ton hot heel, followed by the first basket (containing scrap, DRI fines – defined as  $\leq 3\text{mm}$  material – constituting approximately 8% of the total metallic charge, slag formers and carbonaceous material and pool iron). After charging the basket, the roof is swung closed and the power switched on. Once most of the scrap is molten (heavy scrap can still be left at this stage) the operator takes a "melt-in analysis" of the steel bath. Continuous roof charging of DRI (with some additional slag formers) is subsequently started, while continuing arcing. In total, roof DRI constitutes approximately 40% of the metallic charge. The operator starts blowing carbon and/or oxygen into the melt (after taking another steel sample) to aid the formation of a foaming slag by inducing "CO boil". This process continues until the steel is fully liquid and ready for tapping; one last furnace sample is taken to analyse carbon, nitrogen and oxygen levels. Carbon is adjusted to specification, nitrogen checked (if levels are elevated, the material might be re-classed as a less valuable steel grade) and the oxygen level is used to assess the amount of de-oxidant to be added during tapping. The furnace is subsequently tilted and tapping commences through an eccentric bottom taphole at the back of the furnace. The aim tapping time is less than 3 minutes (on average 2.5 minutes is achieved), to limit slag carryover as well as nitrogen pickup. Following tapping, the liquid steel (containing on average 800-1100 ppm dissolved oxygen) is deoxidised with Al, Si or both.

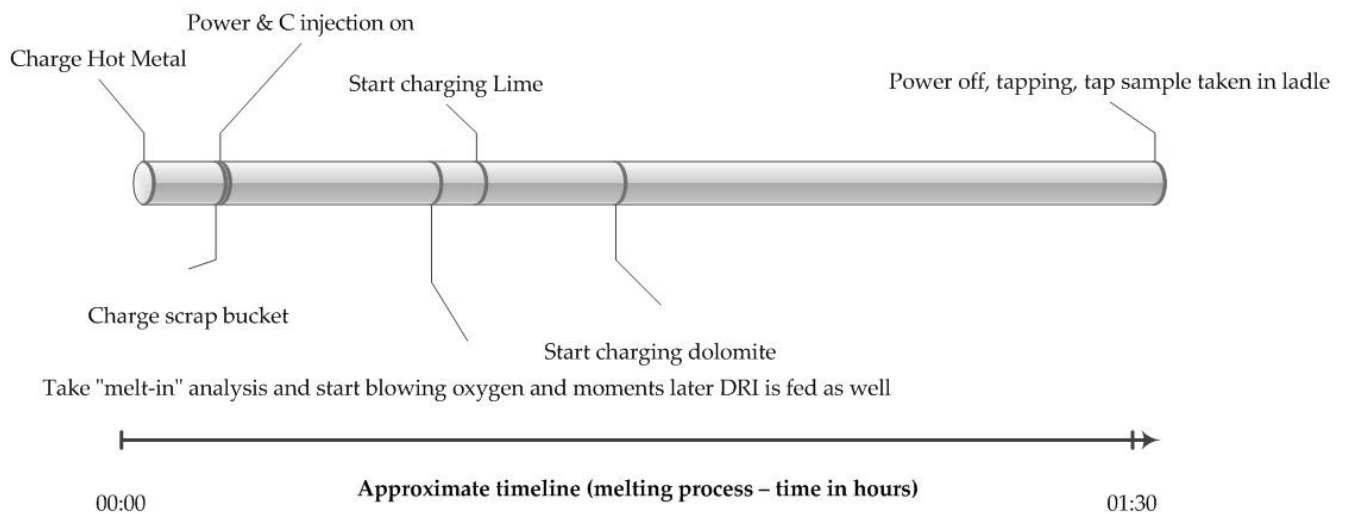


**Fig. 1:** Approximate timeline for steelmaking in the EAF as considered in this project.

## Investigation

Plant data from a typical month's production were analysed to determine relationships between the proportion of DRI charged and tap nitrogen level, and between melt-in carbon and tap nitrogen.

The nitrogen content of samples of SL/RN DRI was determined by combustion analysis. To this end, a composite DRI sample was supplied by plant personnel (approximately 30 kg in total, from two SL/RN kilns). The samples were split into smaller aliquots by cone and quartering, and then separated into different size fractions (in the range  $-25\text{ mm} +212\ \mu\text{m}$ )

using a set of Tyler sieves. Aliquots were taken from each size fraction, and milled in a swing mill for combustion analysis.

## Results and discussion

### *Relationship between DRI input and tap nitrogen*

A month's tap analyses of three furnaces are summarised in Fig. 2. In drawing Fig. 2, only those heats which did not use hot metal were considered, and only considering heats with adequate slag foaming (the plant uses a system which monitors slag foaming; only heats with well-foamed slag for more than 50% were included). Based on these selection criteria, the number of relevant heat analyses was 270 (out of a total of 682 heats).

It was found that when more DRI is charged to the furnace, the nitrogen levels are slightly higher. This is in contrast with general EAF experience, that DRI charged to an EAF dilutes other nitrogen-containing materials (e.g. scrap) to lower the nitrogen content at tap. From Fig. 2, it can be seen that, for this plant, more DRI charged to the furnace (as a percentage of the total metal charge) did not result in a lower tap nitrogen content; the nitrogen content did not decrease along the dilution line (the broken line in Fig. 3) as expected.

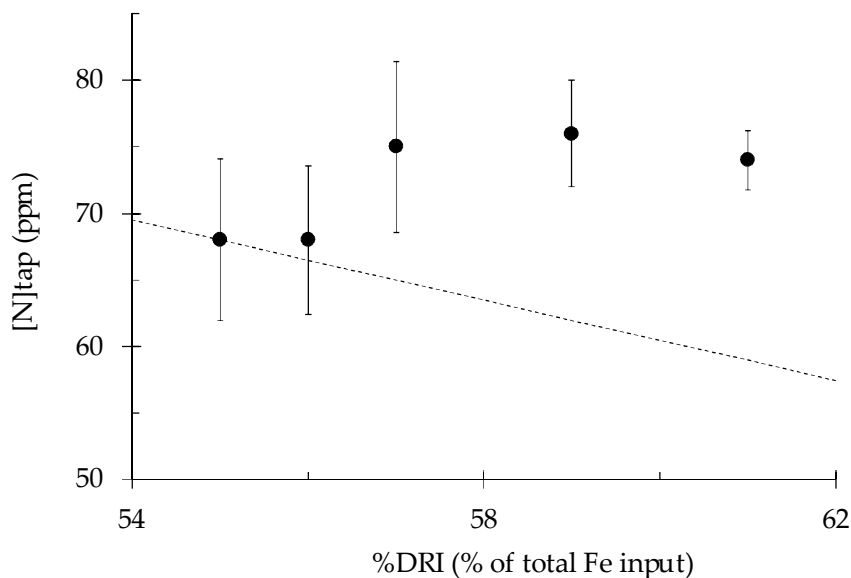


**Fig. 2:** Nitrogen content of liquid steel after tapping from the electric arc furnaces (samples taken directly after tap, before dispatch to the ladle furnace). These are average values, for heats consisting of scrap and DRI only. The broken line shows the expected trend for the case where DRI simply dilutes the nitrogen within the steel melt, for the case where the DRI contains no nitrogen.

### *Nitrogen content of DRI*

Combustion analysis showed that the DRI has a significant nitrogen content (Fig. 3). There is a clear dependence on particle size, with larger DRI particles containing lower amounts of nitrogen. Possible origins of the nitrogen are as follows:

Coal contains some nitrogen: the average nitrogen content of all coals listed in the US Geological Survey Coal Quality Database<sup>9</sup> is 1.3% by mass (dry basis). One published source suggests a somewhat higher concentration (around 2%) in South African coals<sup>10</sup>. When the

coal is devolatilised, N-containing gaseous species (notably HCN) are released<sup>11,12</sup> which could in principle nitride iron. However, volatile release occurs while the solids are heating up before metallic iron has formed:<sup>12</sup> no metallic iron is present to be nitrated when volatile nitrogen-bearing species are released, and nitrogen from coal is hence not expected to be a significant source of the nitrogen in the SL/RN DRI product.

Since the freeboard gas largely consists of nitrogen in both the rotary kiln and the cooler, nitrogen gas diffusion into the porous DRI particles can cause nitriding. Although the solids bed is continuously flushed by CO (reaction product), during reduction in the rotary kiln, and no nitrogen pick-up is expected, the reduction rate rapidly decreases once the DRI is cooled (upon transfer to the rotary cooler), causing CO production to cease and allowing nitrogen to diffuse into the solids bed and into the individual DRI particles. It is hence thought that nitriding of the DRI particles occurs during cooling in the rotary cooler, where the flow of CO from the bed is not sufficient to shield the DRI from nitrogen present in the cooler atmosphere. This suggestion was tested with a simple diffusion model, as presented in the next section.

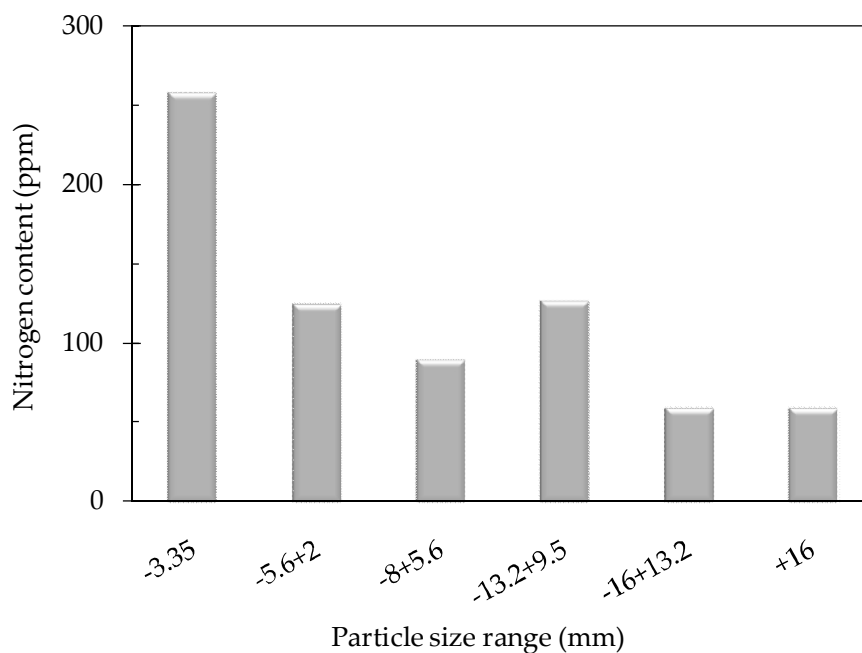


**Fig. 3:** Nitrogen content of different size fractions of SL/RN DRI

*Estimate of nitrogen penetration into the solids bed*

For nitriding of the metallic iron to occur, gaseous nitrogen needs to diffuse into the solids bed (in the rotary kiln or cooler), against the outward flow of carbon monoxide (which is the main gaseous product of the reduction reaction). Detailed analysis of this mass transfer situation would be quite complex, and is beyond the scope of this project: reaction steps include diffusion of nitrogen through the boundary layer between the solids bed and the freeboard, possible entrainment of nitrogen from the freeboard when the solids tumble down the surface of the solids bed (as a result of kiln rotation), diffusion of nitrogen into the solids bed, pore diffusion of nitrogen into the direct-reduced iron, and solid-state diffusion of atomic nitrogen into the metallic iron. Instead of attempting to solve this complex mass transfer situation, a simplified static one-dimensional situation was considered, to test the

basic concept that diffusion of nitrogen into the solids bed is feasible under kiln and cooler conditions.

The approach of Tien and Turkdogan<sup>13</sup>, developed to assess the diffusion of inert gas into metal oxide/carbon mixtures during reduction, was adapted for this purpose. Tien and Turkdogan derived the relevant relationships from the "dusty gas model"; the relationships relevant to diffusion in CO-N<sub>2</sub> mixtures (where the two diffusing species have the same molar mass and hence diffuse at the same rate) are as given below:

The total flux (due to diffusion and bulk gas flow) in the  $z$  direction is as follows:

$$J_i = -D_e \frac{dn_i}{dz} - X_i \frac{\kappa P}{\mu RT} \frac{dP}{dz}$$

where  $D_e$  is the effective diffusion coefficient through the pores of the solids bed,  $dn_i/dz$  is the concentration gradient,  $X_i$  is the mole fraction (note that  $n_i = X_i P / RT$ ),  $\kappa$  is the permeability of the solids bed,  $P$  the absolute pressure,  $\mu$  is the gas viscosity,  $R$  the ideal gas constant and  $T$  the absolute temperature.

The shape of the concentration profile into the solids bed would depend on the relative efficiency of diffusion into the solids bed, and uptake of nitrogen by the iron (through pore diffusion, and diffusion of atomic nitrogen into the austenite). A first estimate of the concentration profile in the solids bed can be obtained by assuming stagnant diffusion of nitrogen, that is,  $J_{N_2} = 0$ . This would be the case if nitrogen uptake by the iron (rather than diffusion into the bed) is rate-determining. For this case, the flux of carbon monoxide out of the bed is then given by<sup>13</sup>:

$$J_{CO} = -\frac{1}{RT} \left( D_e + \frac{\kappa P}{\mu} \right) \frac{dP}{dz}$$

This relationship was applied to a one-dimensional static bed containing iron oxide, iron and carbon, which is undergoing reduction. The temperature was assumed to be uniform within the mixture (as is the case in the bed in the SL/RN kiln<sup>12</sup>), and hence the rate of reaction was assumed to be the same everywhere within the solids bed, generating CO at a rate of  $\dot{N}_V$  mol m<sup>-3</sup> s<sup>-1</sup> (per unit volume of bed). The solids bed was bounded below by an impervious surface, with the upper surface exposed to the nitrogen-containing gas freeboard (see Fig. 4).

For this situation, the flux of CO (in the  $z$  direction) depends on position within the bed, as follows:

$$J_{CO} = -\dot{N}_V (h - z)$$

If it is assumed that the pressure change within the reacting bed is small compared with the total (absolute) pressure, the relative pressure within the bed is found as follows, by integration:

$$\Delta P = \dot{N}_v \frac{RT}{D_e + \frac{\kappa P}{\mu}} (zh - z^2 / 2)$$

The local (steady-state) concentration of N<sub>2</sub> for stagnant diffusion is found from the flux equation, for J<sub>N<sub>2</sub></sub>=0:

$$D_e \frac{dX_{N_2}}{dz} \frac{P}{RT} = -X_{N_2} \frac{\kappa P}{\mu RT} \frac{dP}{dz}; \quad \frac{dX_{N_2}}{dz} = -X_{N_2} \frac{\kappa}{\mu D_e} \frac{dP}{dz}$$

Substitution of the expression for  $\frac{dP}{dz}$  then yields :

$$X_{N_2} = X_{N_2}^o \exp \left[ -\frac{\kappa RT \dot{N}_v}{D_e \mu (D_e + \kappa P / \mu)} (zh - z^2 / 2) \right] = X_{N_2}^o \exp \left[ -\frac{\kappa}{D_e \mu} \Delta P \right]$$

where X<sub>N<sub>2</sub></sub><sup>o</sup> is the mole fraction of nitrogen in the gas freeboard at the surface of the solids bed.

The following input data were used to evaluate the nitrogen concentration:

The binary diffusivity (in CO-N<sub>2</sub> mixtures) was calculated from the equation of Hirschfelder et al.<sup>14,15</sup> Following Tien and Turkdogan,<sup>13</sup> it was assumed that the Knudsen diffusion effect is negligible; hence the effective diffusivity through the pores of the solids bed is given by:

$$D_e = \frac{\varepsilon}{\tau} D_{12}$$

where ε is the void fraction in the solids bed, τ the tortuosity, and D<sub>12</sub> the binary diffusivity. The void fraction was assumed to be approximately 0.4; the tortuosity was estimated from the expression given by Wu et al.<sup>16</sup>, giving τ=1.69, or ε/τ=0.24, which appears reasonable.<sup>17</sup> Gas viscosity was similarly calculated from the Hirschfelder et al.<sup>14,15</sup> correlations, using the values for carbon monoxide.

The permeability was calculated from the Kozeny-Carman equation,<sup>17</sup> assuming spherical particles:

$$\kappa = \frac{d_p^2 \varepsilon^3}{150(1-\varepsilon)^2}$$

where d<sub>p</sub> is the particle diameter. In the calculations a particle diameter of 0.01 m was assumed. (While the predicted pressure drop depends strongly on the particle diameter, the mole fraction of nitrogen within the solids bed was not found to be a strong function of d<sub>p</sub>.)

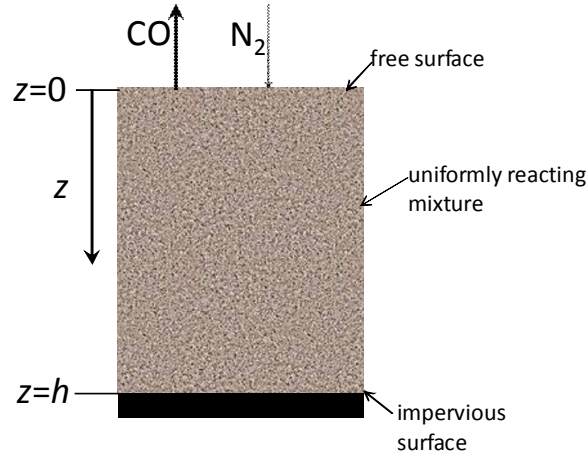


**Fig. 4:** Schematic drawing of the physical situation considered for the dusty-gas calculations.

Ranges of CO generation rate ( $\dot{N}_V$ ) which could be expected under industrial conditions were estimated from the results of Venkateswaran and Brimacombe,<sup>12</sup> for the Griffith kiln (length 125 m, internal diameter 5.5 m). The reduction profile from that work was used to calculate the reduction rate at different positions in the kiln, as shown in Fig. 5, using the following values from Venkateswaran and Brimacombe:<sup>12</sup> a degree of fill of 0.2, Fe feed rate of 1036 t day<sup>-1</sup> (based on a pellet feed rate of 1570 t day<sup>-1</sup>, and an assumed pellet Fe content of 66%), a molar ratio of O to Fe in the pellets of 1.5, and a concentration of Fe in the solids bed of 763 kg m<sup>-3</sup>. As the figure shows, the CO generation rate peaks at approximately 1.6 mol m<sup>-3</sup>s<sup>-1</sup>, and decreases to approximately one-tenth this value towards the discharge end. In the rotary cooler, the CO generation rate would be even lower, as the temperature drops and CO formation (through reaction of CO<sub>2</sub> with the coal) slows. Hence three CO generation rates were considered: 1 mol m<sup>-3</sup>s<sup>-1</sup> (representative of the main reduction zone at the centre of the kiln), 0.1 mol m<sup>-3</sup>s<sup>-1</sup> (representative of the conditions towards the discharge end of the kiln), and 0.01 mol m<sup>-3</sup>s<sup>-1</sup> (assumed to be representative of conditions in the cooler). The bed temperature was taken to be 1000°C in the kiln, and 900°C in the cooler (it was found that the calculated nitrogen concentration profile changes little if the assumed temperature changes, though). The nitrogen content of the gas at the bed surface was taken to be 65% (corresponding to full combustion of pure CO with air). The ambient pressure was taken to be 1 atm. The bed depth ( $h$  in Fig. 6) was taken to be half the maximum depth of the bed in the rotary kiln (since the bed in the kiln is in the shape of a circular segment, its depth varies from zero up to a maximum depth of 1.4 m, for the Griffith kiln).

Fig. 6 shows that essentially no nitrogen penetration into the solids bed is expected halfway along the rotary kiln (where the reaction rate is high), with some penetration towards the kiln exit, and significant penetration in the cooler. The pressure increase within the bed can be seen to be affected mainly by the reaction rate, and secondarily by the temperature difference between the kiln and cooler. As a measure of the degree of nitrogen penetration, the position within the bed was determined where the partial pressure of nitrogen in the gas phase would be in equilibrium with 50 ppm of dissolved nitrogen in the austenite, based on the literature values for nitrogen solubility<sup>18</sup> (the value of 50 ppm is an arbitrary one, but chosen to reflect a significant nitrogen pick-up). Based on this criterion, the depth of nitrogen penetration into the solids bed at the centre of the kiln is estimated to be 2.2 mm (that is, less than the diameter of the solid particles), compared with 22 mm towards the kiln exit, and 267 mm in the cooler. These values emphasise that the nitrogen penetration depth is approximately



inversely proportional to the CO generation rate, and that significant nitrogen penetration into the solids bed is expected close to the kiln exit, and certainly in the rotary cooler.

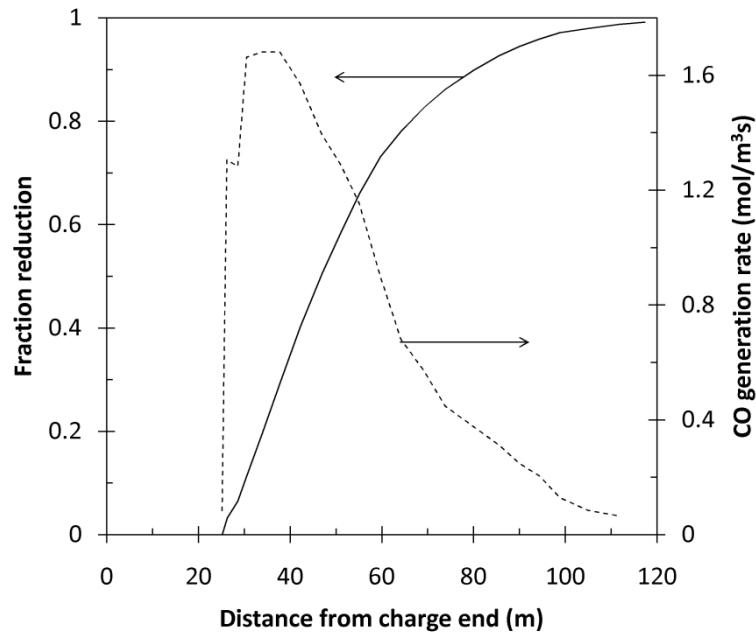


**Fig. 5:** Volumetric generation rate of CO in a SL/RN rotary kiln (broken line) as calculated from the reduction profile as reported by Venkateswaran and Brimacombe<sup>12</sup> (solid line).

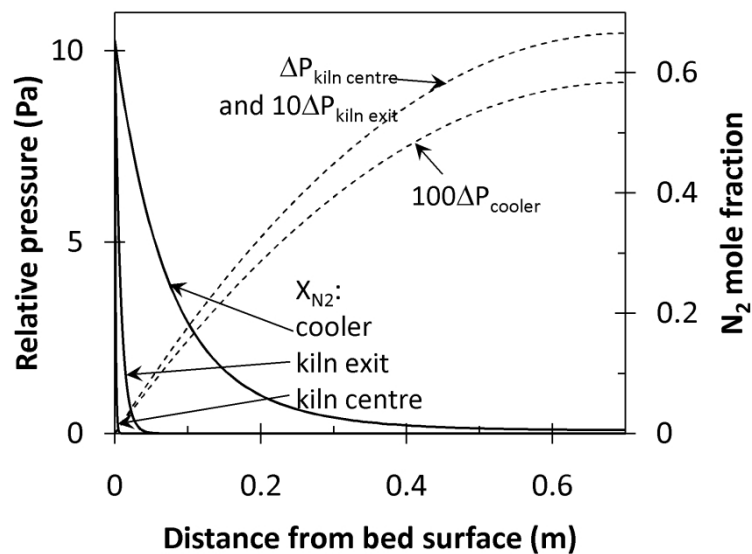


**Fig. 6:** Calculated pressured drop (broken lines; pressure drop for kiln exit and cooler multiplied by 10 and 100 respectively to show these on the same graph) and nitrogen mole fraction, within the solids bed at different positions in the SL/RN process.

#### *Possible approaches to nitrogen control*

The results presented in the previous sections show that significant amounts of nitrogen in EAF raw materials lead to higher nitrogen levels at tap; and that direct reduced iron produced in SL/RN rotary kilns was found to contain as much as 250 ppm N, in contrast with previous assumptions of low nitrogen levels. This is exacerbated by the low carbon content of this type of DRI, too low to enhance carbon boil and slag foaming.

Carbon in the steel bath can contribute considerably to nitrogen control, by CO flushing of the bath. This proposed mechanism is supported by data from the plant considered here. Fig. 7 presents a scatter plot of the final nitrogen content of steel tapped plotted against melt-in carbon content as measured after scrap melting (data from 3120 heats, with no filtering of the data, i.e. the heats with hot metal are included). While the scatter plot does not show a clear trend, grouping the data (based on the carbon content) and calculating the mean tap nitrogen (with 95% confidence interval on the mean) each group does reveal a strong relationship (Fig. 8).

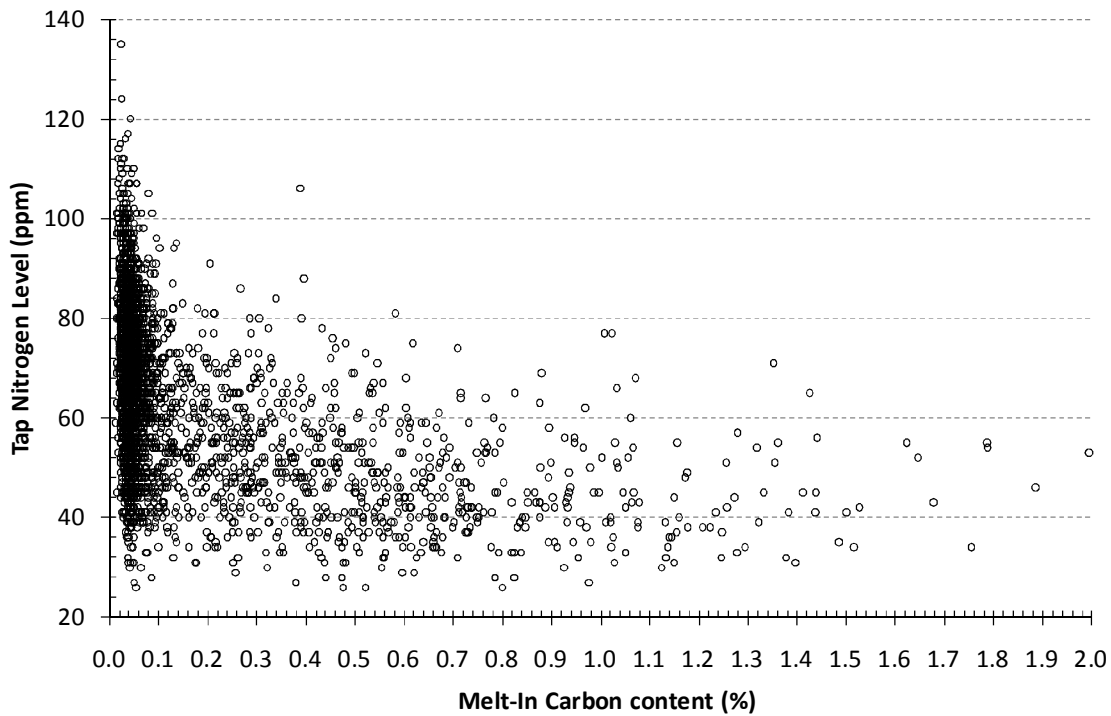


**Fig. 7:** Scatter plot of nitrogen content at tap vs. melt-in carbon content

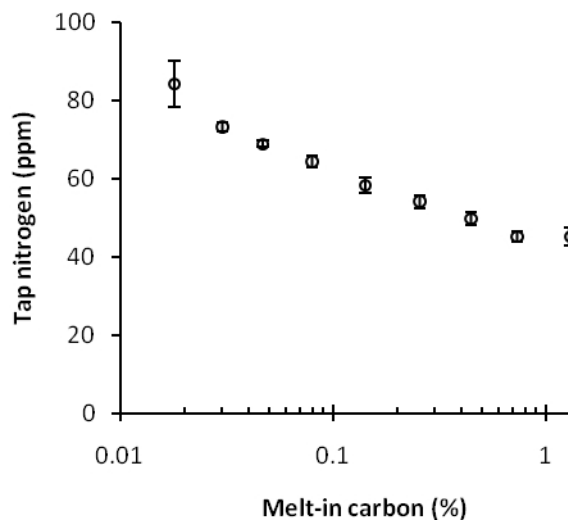


**Fig. 8:** Mean nitrogen content of tapped steel (with 95% confidence intervals); heats grouped by melt-in carbon content

Fig. 8 shows that to control the average nitrogen content of steel to below 50 ppm, the carbon content at melt-in should be approximately 0.2-0.3% C. To achieve the required melt-in carbon content, the carbon should be preferably charged in the basket. There have been suggestions of carburising SL/RN DRI at the plant, to increase its carbon content – but this option is unlikely to be effective, since most of the DRI is charged through the roof of the furnace. Goldstein et al. showed that in order to realise the benefits of carbon in DRI, it cannot be charged through the roof after slag has formed<sup>4</sup> – the low density of DRI, lower than that of slag, does not allow for deep penetration required for removal of nitrogen from a steel melt.

SL/RN DRI can be briquetted; as showed in early reports on development of the SL/RN process,<sup>19</sup> - a pressure of approximately 350 MPa during briquetting produced briquettes with a maximum density around 5 t m<sup>-3</sup>, sufficient to penetrate the slag layer. In this case, carburisation of DRI would also be necessary if an increase in melt carbon is to be obtained.

It is hence concluded that carburisation of DRI (which would require installing a carburisation system at the plant, using, for example, coke oven gas) would not necessarily benefit the EAF steelmaking process, unless the majority of the DRI were charged in the basket, or briquetting were implemented.

In contrast, the role of carbon boil in removing nitrogen is well established,<sup>20</sup> and supported by the strong role of melt-in carbon demonstrated in this work. Previously reported plant data indicated that a minimum of 0.3% C removal is required for adequate nitrogen removal through the carbon boil mechanism.<sup>20</sup> This required carbon level agrees with the plant data from the current work, shown in Fig. 8.

## Conclusion

Direct reduced iron produced in SL/RN rotary kilns was found to contain as much as 250 ppm nitrogen, in contrast with previous assumptions of low nitrogen levels. Nitrogen is suspected to be picked up during cooling of DRI in a rotary cooler, where the flow of CO gas from the bed is low and penetration of nitrogen from the cooler atmosphere is possible. Carbon boil during electric furnace steelmaking is efficient at lowering the nitrogen level; to utilise this to achieve a nitrogen level at tap of 50ppm or less, the melt-in carbon needs to be 0.2-0.3% or higher.

## Acknowledgements

The authors thank AMSA staff for samples, data and information, as well as the Department of Materials Science and Metallurgical Engineering of the University of Pretoria for financial support.

## References

1. "2010 World Direct Reduction Statistics". Available at [www.midrex.com](http://www.midrex.com) (last accessed 18 August 2011).
2. D. Trotter, D. Varcoe, R. Reeves and S. Hornby Anderson: *SEAFISI Q.*, 2002, 31(2), 39-50.
3. P.J. Koros: AISTech 2005 Proceedings, Vol. 1, Charlotte, North Carolina, USA, 9-12 May 2005, pp. 395-402.

4. D.A. Goldstein, R.J. Fruehan and B. Ozturk: *Iron Steelmaker*, 1999, 26(2), 49-61.
5. J.A.T. Jones: *Electr. Furn. Conf. Proc.*, 1998, 56, 457-478.
6. D. Anghelina, G.A. Irons and G.A. Brooks: AISTech 2005 Proceedings, Vol. 1, Charlotte, North Carolina, USA, 9-12 May 2005, pp.403-412.
7. B. Strohmeier and W. Peters: *Metall. Ital.*, 1988, 80(11), 849-859, 892.
8. B. Anameric and S.K. Kawatra: *Miner. Process. Extr. Metall. Rev.*, 2007, 28, 59-116.
9. "U.S. Geological Survey Open-File Report 97-134: U.S. Geological Survey Coal Quality Database: Version 2.0". Available at <http://energy.er.usgs.gov/coalqual.htm> (last visited 18 August 2011)
10. R. Falcon and A.J Ham: *J. South. Afr. Inst. Min. Metall.*, 1988, 88, 145-161.
11. P. Abelha, I. Gulyurtlu, and I. Cabrita: *Energy Fuels*, 2008, 22, 363-371.
12. V. Venkateswaran and J.K. Brimacombe: *Metall. Trans. B*, 1977, 8B, 387-398.
13. R.H. Tien and E.T. Turkdogan: *Metall. Trans. B*, 1977, 8B, 305-313.
14. J.O. Hirschfelder, R.B. Bird and E.L. Spatz: *J. Chem. Phys.*, 1948, 16, 968-981.
15. J.O. Hirschfelder, R.B. Bird and E.L. Spatz: *Chem. Rev. (Washington, DC, U. S.)*, 1949, 44, 205-231
16. J. Wu, B. Yu and M. Yunj: *Transp. Porous Media*, 2008, 71, 331-343.
17. W.L. McCabe, J.C. Smith and P. Harriott: "Unit operations of chemical engineering", 6th edn., 159, 858; 2001, McGraw-Hill.
18. S. Ban-ya and Y. Iguchi: in "Steelmaking Data Sourcebook", (ed. The Japan Society for the Promotion of Science, The 19th Committee on Steelmaking), 27-34; 1988, Gordon and Breach Science Publishers.
19. J.G. Sibakin: General Meeting of the American Iron and Steel Institute, New York, NY, USA, 23 May 1962, pp. 1-42.
20. C.F. Pilliod: *Electr. Furn. Conf. Proc.*, 1986, 46, 107-110.